Electronic Supplementary Material (ESI) for Journal of Materials Chemistry A.

Electronic Supplementary Information for

IL-induced formation of dynamic complex-iodine anions in IL@MOF composites for efficient iodine capture

Yuanzhe Tang,[a] *Hongliang Huang,**[b] *Jian Li,*[a] *Wenjuan Xue,*[b] *and Chongli Zhong**[a,b]

[a] State Key Laboratory of Organic-Inorganic Composites, Beijing University of Chemical Technology, Beijing 100029, China

[b] State Key Laboratory of Separation Membranes and Membrane Processes, School of Chemistry and Chemical Engineering, Tianjin Polytechnic University, Tianjin 300387, China.

E-mail: huanghongliang@tjpu.edu.cn, zhongchongli@tjpu.edu.cn

1.Experimental Section

Materials

All the reagents and solvents are commercially available and used without further purification. Aluminum chloride hexahydrate ($AlCl_3 \cdot 6H_2O$, 99.9%) was purchased from J&K. *p*-Tolunitrile (99%), trifluoroacetic acid and trifluoromethanesulfonic acid (99%) were purchased from Energy Chemical Co. Ltd. Sodium hydroxide (NaOH, 99%) was purchased from Beijing Chemical Works. N, N-Dimethylformamide was purchased from Sinopharm Chemical Reagent Co. Ltd. Acetone, toluene, methanol and concentrated nitric acid was purchased from Beijing Chemical Works. N-methylimidazole and 1-bromobutane were purchased from Energy Chemical Co. Ltd.

Equipment

All the reactions were performed under ambient atmosphere using oven-dried glassware unless otherwise mentioned. Fourier transform infrared spectroscopy (FT-IR) analysis was performed on a Nicolet 6700 FT-IR spectrophotometer. Spectra were recorded in the 4000 to 400 cm^{-1} wavenumber range. Nuclear magnetic resonance (NMR) experiments were carried out on a Bruker Avance III 400 MHz. X-ray photoelectron spectroscopy (XPS) was recorded on a Kratos ASAM800 spectrometer. Powder X-ray diffraction data (PXRD) analysis of powders were recorded on a SHIMADZU XRD-6000-X-ray diffractometer in reflection mode using Cu Ka radiation (λ=1.5406 Å). The 2θ range from 1˚ to 50˚ was scanned with a step size of 0.01˚. The powders morphologies were observed via scanning electron micrographs (SEM) (S-4800). The gold-coated specimens were fabricated under an acceleration voltage of 10–20 kV. The surface areas and pore properties were investigated by nitrogen adsorption and desorption at 77 K using ASAP 2020 Plus HD88. The pore-size-distribution curves were obtained from the adsorption branches using the density functional theory (DFT) method. Thermogravimetric analysis (TGA) data were recorded by using a TGA-50 (SHIMADZU) thermogravimetric analyzer with a heating rate of 10 °C min^{-1} under N_2 atmosphere. Element analyses (EA) were performed on a CARLO ERBA 1106. Raman spectra were obtained using an Xplora PLUS Raman microscope (Horiba Company) with a 785 nm laser and a 1200 lines/mm grating. The acquisition time was 10 s and accumulated for 5 cycles. UV−vis spectra were recorded on a Shimadzu UV-2600 spectrometer.

Synthesis of H_3TATB

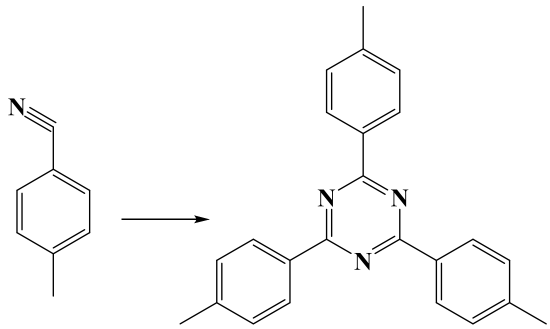

1

2, 4, 6-tri-*p*-tolyl-*s*-triazine (1): 2, 4, 6-tri-*p*-tolyl-*s*-triazine was prepared according to the previous literature[1]. *p*-Tolunitrile (2.9 mL, 24.3 mmol) was added slowly to trifluoromethanesulfonic acid (10 g). The mixture was stirred for 13 hours, poured on ice and neutralized with sodium hydroxide solution (1M, 25mL). The precipitate was collected by filtration and then washed with water and acetone. Recrystallization in toluene gave the title compound as white crystals (2.66 g, yield: 94 %). ^{1}H-NMR (400 MHz, $CDCl_3$): δ 8.65 p.p.m. (d, J = 8.1 Hz, 6H), 7.36 (d, J = 8.1 Hz, 6H), 2.45 (s, 9H);.

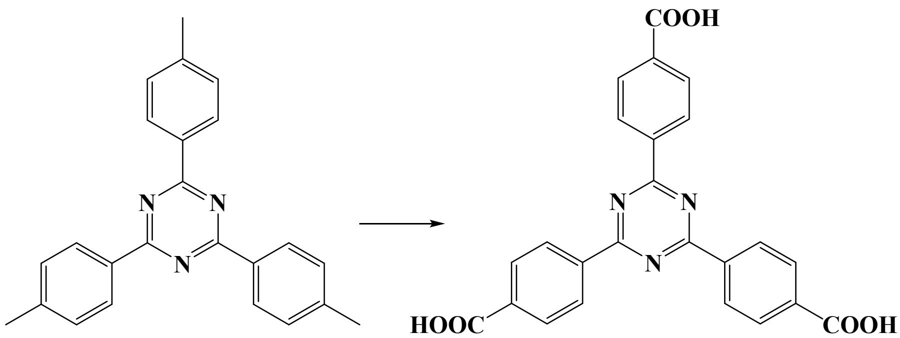

1 2

4,4',4"-*s*-trizaine-2,4,6-triyltribenzoic acid (2): 2,4,6-tri-*p*-tolyl-*s*-triazine (1g, 2.21mmol) was added to concentrated nitric acid (3 mL) and water (9 mL) in the Teflon reactor. The mixture was heated for 24 hours, the resulting mixture was cooled to room temperature and then the suspension was filtered. Recrystallization in N, N-Dimethylformamide gave the title compound as the yellowish solid (0.92g, yield: 92%). ^{1}H-NMR (400 MHz, DMSO-d_6): δ 13.30 p.p.m. (br, 3H), 8.65 (d, J = 8.2 Hz, 6H), 8.08 (d, J = 8.2 Hz, 6H).

Synthesis of PCN-333(Al)

PCN-333(Al) was prepared according to the previous literature.[2] H_3TATB (50 mg) and $AlCl_3 \cdot 6H_2O$ (200 mg) were dissolved in 10 ml DMF, then 1.0 ml trifluoroacetic acid was added. The mixture was heated up at 135 °C in an oven for 2 days until white precipitate formed. The white precipitate was centrifuged and washed with fresh DMF and acetone for several times. Yield (based on ligand): 80%.

Synthesis of IL@PCN-333(Al)

N-methylimidazole (1.5g) was added to a vial containing dehydrated PCN-333(Al) (0.3 g) and was magnetically stirred at room temperature for 24 h. After that, 1-bromobutane (2.8 g) (the molar amount slightly more than N-methylimidazole) was added to the mixture and magnetically stirred for an additional 24 h at room temperature. The resulting solid was separated via filtration and washed with ethanol three times. Finally, the resulted solid product was dried in an oven at 80 °C overnight at vacuum.

Synthesis of MIL-101(Cr)

MIL-101(Cr) was prepared according to the previous literature.[3]

Synthesis of IL@MIL-101(Cr)

IL@MIL-101(Cr) composite was systhesized with the similar method of IL@PCN-333(Al). N-methylimidazole (1.5 g) was added to a vial containing dehydrated MIL-101(Cr) (0.3 g) and was magnetically stirred at room temperature for 24 h. After that, 1-bromobutane (2.8 g) (the molar amount slightly more than N-methylimidazole) was added to the mixture and magnetically stirred for an additional 24 h at room temperature. The resulting solid was separated via filtration and washed with ethanol three times. Finally, the product was dried in an oven at 80 °C overnight at vacuum.

^{1}H-NMR measurement

0.5 g potassium hydroxide and 10mL D_2O were put into the vial for ultrasound until dissolved to make potassium hydroxide solution. 5 mg sample (IL@PCN-333(Al)) and 1 mL potassium hydroxide solution were loaded into 10 mL centrifuge tube and heated at 80 °C until dissolved.

After being filtered by filter membrane, the solution was injected into nuclear magnetic tube for ^{1}H-NMR measurement.

Iodine Vapor capture

The iodine vapor adsorption capacities of IL@PCN-333(Al) were calculated by mass measurements. Before the iodine adsorption experiment, the ethanol-exchanged samples were heated under vacuum for 12 h at 80 °C. The degassed sample was then transferred into a glass vial, which contained a small amount of solid I_2 in an open vessel and the vessel charged with at atmospheric pressure. The vessel was then sealed and heated at 75 °C for 0.5−48 h to allow adsorption of iodine into the desolvated MOF. The iodine-loaded samples were cooled to room temperature and collected for further analysis. The iodine capture of IL@PCN-333 (Al) was evaluated by the following equation:

$$(W2 - W1)/W1 * 100 \text{ wt.\%}$$

Where W_1 and W_2 represent the mass of IL@PCN-333 (Al) before and after iodine capture, respectively.

Iodine adsorption kinetics measurement

IL@PCN-333(Al) sample (0.015 g) was added into a glass vial containing 10 ml stock solution of iodine with the concentration of 1.6 mg/mL. The mixture was kept at room temperature for 48 h. During the adsorption period, the mixture was filtered at intervals through a membrane filter for all samples. Subsequently, the filtrates were collected and measured by using UV-2600 to determine the residual iodine content.

Iodine adsorption isotherm measurement

IL@PCN-333(Al) sample (0.015 g) was added into a glass vial containing 10 ml stock solution of iodine with different concentrations (0.26-6.35 mg/mL). The mixture was kept at room temperature for 48 h and filtered through a membrane filter for all samples. Subsequently, the filtrates were collected and measured by using UV-2600 to determine the residual iodine content.

Regeneration of Adsorbents

The I_2-IL@PCN-333(Al) used in adsorption measurements were washed with n-hexane (by a proportion of 300 mL n-hexane per 30 mg IL@PCN-333(Al)) through soaking overnight under stirring at room temperature for 12 h. This procedure was repeated at least three times by using fresh n-hexane. After filtration, the wet products were dried under vacuum at 348 K for 1 h to remove the residual solvents. The regenerated IL@PCN-333(Al) were used again for the iodine adsorption at least three cycles.

The distribution coefficient of the Adsorbent

The distribution coefficient (K_d) value in IL@PCN-333(Al) for iodine adsorption was calculated according to the following equation,

$$K_d = \frac{C_0 - C_e}{C_e} \times \frac{V}{m}$$

where C_0 and C_e are the initial and equilibrium concentrations, respectively, V is the volume of solution (mL), and m is the mass of adsorbent used (g)

Computational Models and Methods

To investigate the interaction energies between BrI_4^- /I_2 and the cation of IL, the first principles Density Functional Theory (DFT) calculations were performed using Gaussian 09 program[4]. Møller−Plesset second-order perturbation (MP2) on the Hartree−Fock (HF) self-consistent field (SCF) were calculated. The basis set SDD was employed for the I and Br atoms while 6-31G(d) was used for the rest of the atoms. On the basis of the optimized structures, the single-point energy calculation was performed at a more precise level of MP2/6-311++G(d) ~ SDD. In this level, the SDD functional was used for the I and Br atoms and the basis sets for describing other atoms was replaced by 6-311++G(d)

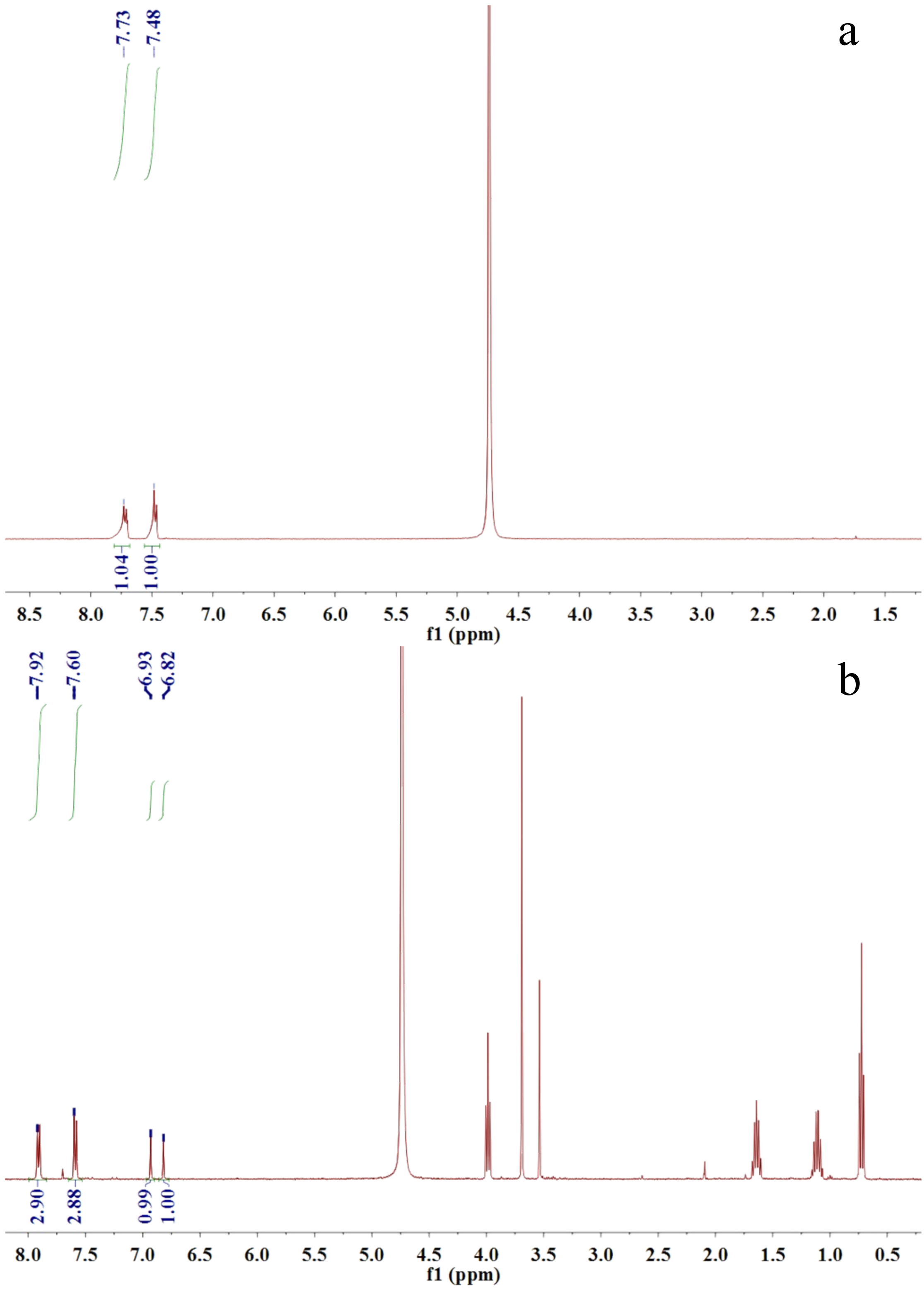

Fig. S1 ^{1}H NMR spectra of (a) pristine PCN-333(Al) and IL@PCN-333(Al)

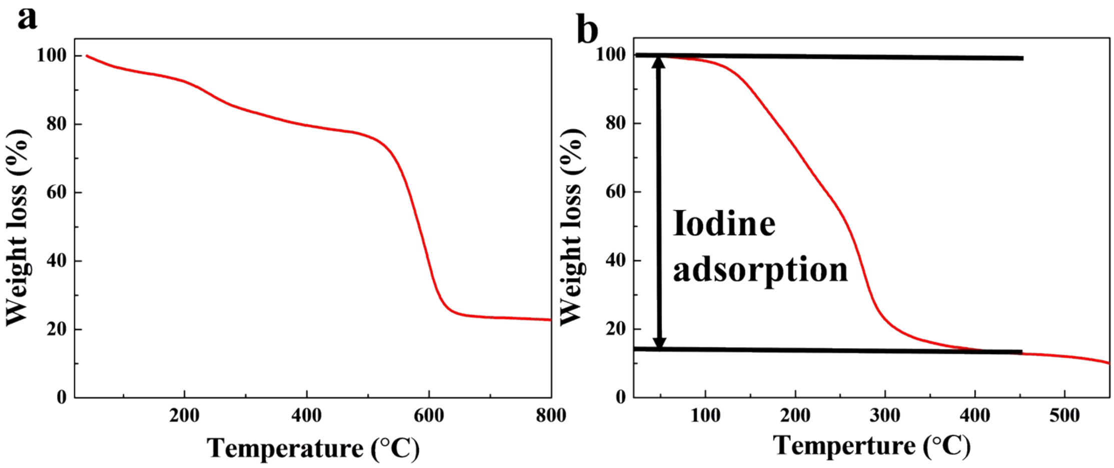

Fig. S2 TGA curves of IL@PCN-333(Al) and I_2-IL@PCN-333(Al).

Table S1 Comparison of iodine vapor adsorption in different materials

No.	Name	BET surface area (m^2/g)	Pore volume (cm^3/g)	Iodine uptake (g/g)	Ref.
1	CalP2	596	0.73	0.88	*5*
2	CalP2-Li	274	0.31	1.08	*5*
3	CalP3	630	0.639	1.96	*5*
4	CalP4	759	1.08	2.2	*5*
5	CalP3-Li	308	0.558	2.48	*5*
6	CalP4-Li	445	0.588	3.12	*5*
7	CMPN-1	230	0.14	0.97	*6*
8	CMPN-2	339	0.39	1.1	*6*
9	CMPN-3	1368	2.36	2.08	*6*
10	CX4-NS	468	0.52	1.14	*7*
11	AC2	824	-	1.17	*8*
12	AC1	1323	-	1.41	*8*
13	MFM-300(Fe)	-	-	1.29	*9*
14	MFM-300(Sc)	-	-	1.54	*9*
15	pha-H_COP-1	217.31	1.048	1.31	*10*
16	S2-LDH	-	-	1.32	*11*
17	S6-LDH	-	-	1.43	*11*
18	S4-LDH	-	-	1.55	*11*
19	NBDP-CPP	658	0.92	1.5	*12*
20	BDP-CPP-1	635	0.78	2.83	*12*
21	BDP-CPP-2	235	0.18	2.23	*12*

22	TTPT	315.5	0.232	1.53	*13*
23	HCMP-1	430	0.22	1.59	*14*
24	HCMP-2	153	0.06	2.81	*14*
25	HCMP-3	82	0.08	3.16	*14*
26	Cu-BTC	-	-	1.75	*15*
27	NTP	1067	0.74	1.8	*16*
28	SCMP-1	413	0.23	1.88	*17*
29	SCMP-2	855	1.5	2.22	*17*
30	NRPP-1	1579	0.91	1.92	*18*
31	NRPP-2	1028	0.81	2.22	*18*
32	NiP-CMP	2600	2.288	2.02	*19*
33	NiMoS	490	1.33	2.25	*20*
34	ZnSnS	400	0.77	2.25	*20*
35	PAF-25	262	-	2.6	*21*
36	PAF-23	82	-	2.71	*21*
37	PAF-24	136	-	2.76	*21*
38	TTA-TFB	1163	0.55	2.7	*22*
39	TFBCz-PDA	1441	0.74	3.7	*22*
40	ETTA-TPA	1822	0.95	4.7	*22*
41	TTA-TTB	1733	1.01	5	*22*
42	TPB-DMTP	1927	1.28	6.3	*22*
43	AzoPPN	400	0.68	2.9	*23*
44	Tm-MTDAB	2.778	0.007	3.06	*24*
45	TTDAB	1.643	0.125	3.13	*24*
46	TTPPA	512	0.3	4.9	*24*
47	SCMP-II	119.76	0.61	3.45	*25*
48	POP-1	12	0.15	3.57	*26*

49	POP-2	41	0.12	3.82	*26*
50	TPT-DHBD$_{100}$	-	-	3.88	*27*
51	TPT-DHBD$_{75}$	-	-	4.12	*27*
52	TPT-DHBD$_{50}$	-	-	4.3	*27*
53	TPT-DHBD$_{25}$	-	-	4.65	*27*
54	TPT-DHBD$_{0}$	-	-	5.43	*27*
55	TTPB	222	0.127	4.43	*28*
56	COF-DL229	1762	0.64	4.7	*29*
57	NCMP1	58	0.15	2.15	*30*
58	NCMP2	280	0.30	1.86	*30*
59	NCMP3	485	0.57	1.61	*30*
60	TPT-Azine-COF	1020	0.65	2.19	*31*
61	TPT-TAPB-COF	957	0.57	2.25	*31*
62	MelPOP-2	50.5	0.22	4.5	*32*
63	TatPOP-2	36.5	0.18	2.62	*32*
64	COGF	-	-	1.4	*33*
65	NOP-53	744	0.73	1.77	*34*
66	NOP-54	1178	1.32	2.02	*34*
67	NOP-55	526	0.42	1.39	*34*
68	AK-1	1634	0.80	2.37	*35*
69	AK-2	2751	1.34	2.62	*35*

70	AK-3	2016	1.04	2.53	*35*
71	3D-PPy	16	-	1.6	*36*
72	P-PPy	6	-	0.63	*36*
73	APOP	490	0.435	2.2	*37*
74	TTPA	308	0.34	4.92	*38*
75	TTDATA	491	0.24	4.72	*38*
76	TTMDATA	456	0.20	4.49	*38*
77	Azo-Trip	510.4	0.47	2.38	*39*
78	HKUST-1@PES	1250	-	5.38	*40*
79	HKUST-1@PEI	990	-	4.98	*40*
80	HKUST-1@PVDF	1100	-	3.75	*40*
81	HKUST-1	1370	-	3.06	*40*
82	NiL_2Cl_2	-	-	0.217	*41*
83	PHF-1	1046	0.61	3.05	*42*
84	PHF-1-Ct	690	0.44	4.05	*42*
85	CTF-CTTD-400	1684	1.44	3.57	*43*
86	CTF-CTTD-500	1334	1.40	3.87	*43*
87	FCMP-600@1	551	0.3865	1.08	*44*
88	FCMP-600@2	636	0.6983	1.41	*44*
89	FCMP-600@3	692	0.4074	0.9	*44*

90	FCMP-600@4	88	0.118	1.11	*44*
91	NT-POP@800-1	499	0.239	0.68	*45*
92	NT-POP@800-2	630	0.433	1.92	*45*
93	NT-POP@800-3	475	0.187	0.56	*45*
94	NT-POP@800-4	736	0.463	1.49	*45*
95	NT-POP@800-5	643	0.602	1.52	*45*
96	NT-POP@800-6	712	0.517	0.95	*45*
97	SCMP-600@1	362	-	1.48	*46*
98	SCMP-600@2	512	-	1.67	*46*
99	SCMP-600@3	642	-	2.04	*46*
100	Azo_{TPE}-CMP	366	1.072	1.08	*47*
101	Ag@Azo_{TPE}-CMP	47	0.110	2.02	*47*
102	MOF “1”	-	-	0.485	*48*
103	MoSx aerogel	-	-	1	*49*
104	CalPOF-1	303	-	4.77	*50*
105	CalPOF-2	154	-	4.06	*50*
106	CalPOF-3	91	-	3.53	*50*
107	MBM	62	0.624	0.98	*51*
108	SIOC-COF-7	618	0.41	4.81	*52*

109	m-CuBTC-0	1281	0.64	0.254	*53*
110	m-CuBTC-0.5	1059	0.51	0.346	*53*
111	m-CuBTC-1	526	0.47	0.437	*53*
112	m-CuBTC-2	596	0.49	0.641	*53*
113	m-CuBTC-0-0.1	1160	0.52	0.642	*53*
114	m-CuBTC-0-0.5	392	0.22	0.739	*53*
115	m-CuBTC-2-0.1	436	0.33	0.749	*53*
116	m-CuBTC-2-0.5	256	0.17	1.061	*53*
117	Complex **1**	168	-	2.16	*54*
118	NH_2-HMONs	421	0.08	2.2	*55*
119	PTPATTh	594	1.469	3.13	*56*
120	PTPATCz	894	1.654	2.54	*56*
121	HCP	1883	2.55	4.27	*57*
122	33PEI@HCP	900	0.73	4.82	*57*
123	50PEI@HCP	707	0.58	5.11	*57*
124	60PEI@HCP	538	0.45	6.07	*57*
125	$\{[Ni_4(44pba)_8]$ sol$\}_n$	-	-	1.1	*58*
126	Cg-5C	387	2.38	2.39	*59*
127	Cg-5P	287	1.62	0.871	*59*
128	Por-Py-CMP	1014	0.81	1.3	*60*

129	JLNU-4	64	-	0.6367	*61*
130	HCPs	584	0.41	4.6	*62*
131	graphene	523	0.31	1.7	*63*
132	PG-600	1064	0.63	2.46	*63*
133	PG-700	1264	0.80	3.46	*63*
134	PG-800	1755	1.31	4.11	*63*
135	**PCN-333(Al)**	**2935.3**	**2.97**	**4.42**	***This work***
136	**IL@PCN-333(Al)**	**1635.3**	**1.40**	**7.35**	***This work***

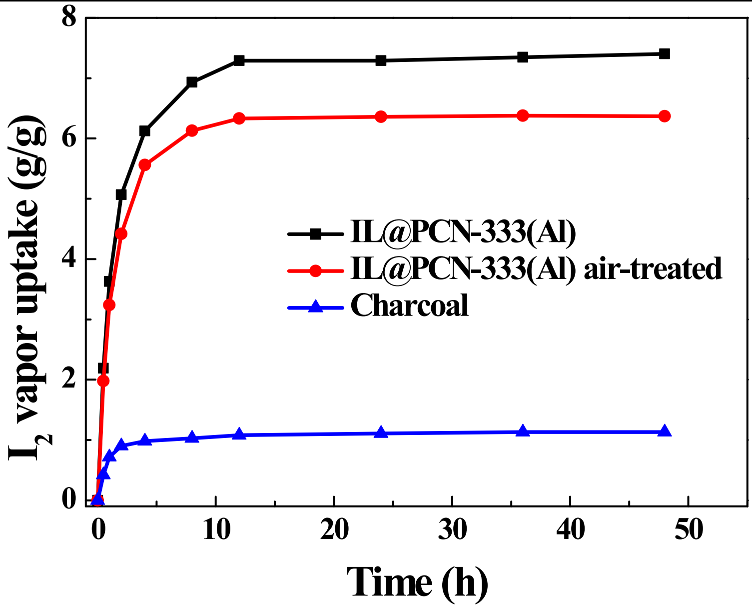

Fig. S3 Gravimetric measurement of iodine vapor capture capacity of IL@PCN-333(Al), air-treated IL@PCN-333(Al) and charcoal as a function of time at 348 K and ambient pressure.

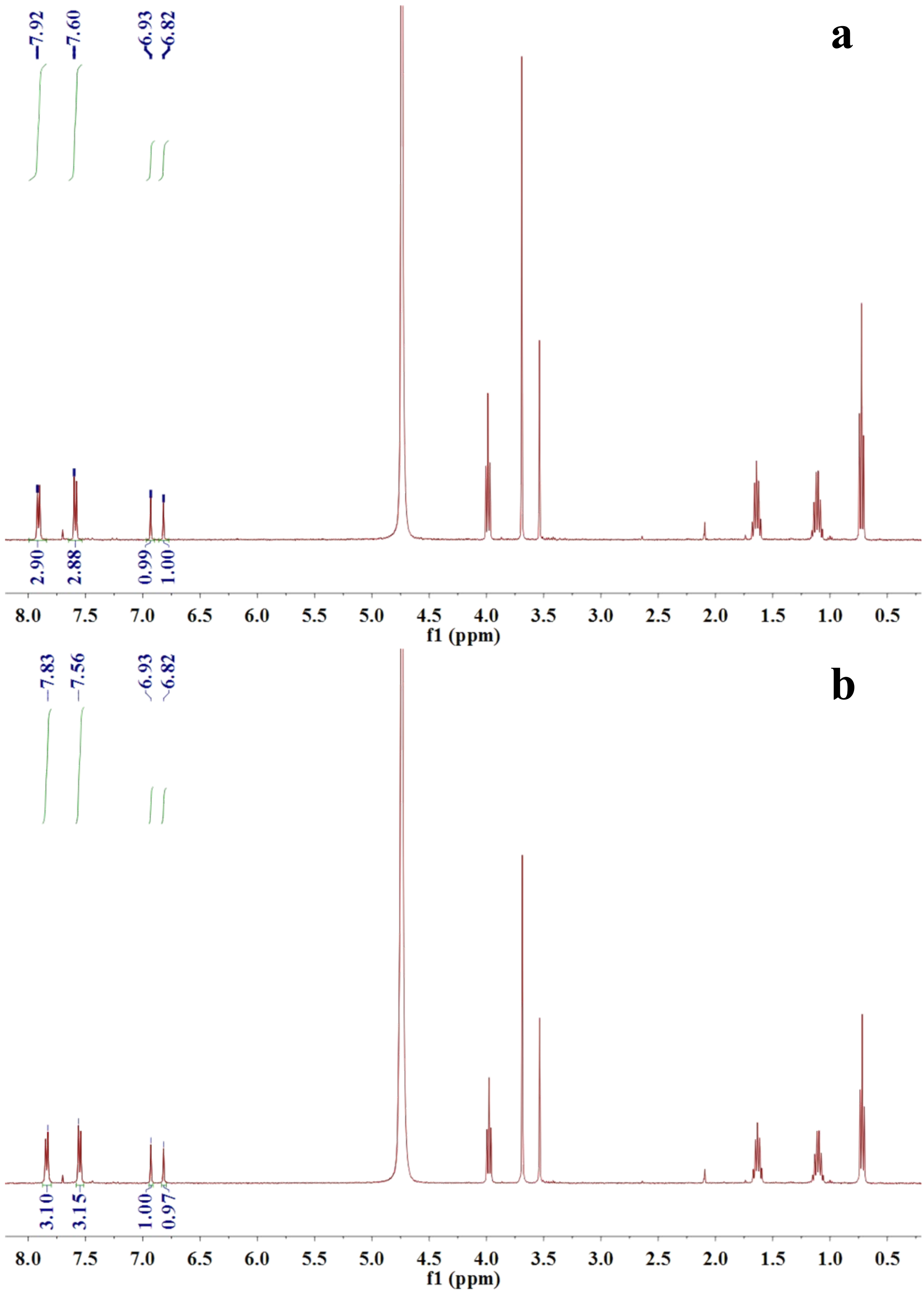

Fig. S4 ^{1}H NMR spectra of (a) IL@PCN-333(Al) was treated before hexane; (b) IL@PCN-333(Al) was treated after hexane.

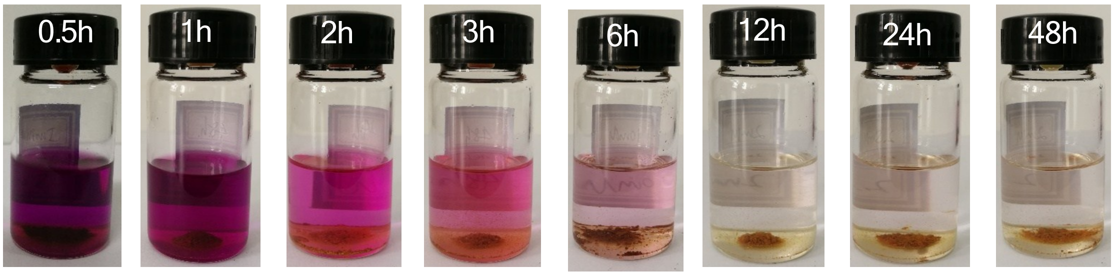

Fig. S5 Photographs to show the color change of adsorption kinetics for IL@PCN-333(Al).

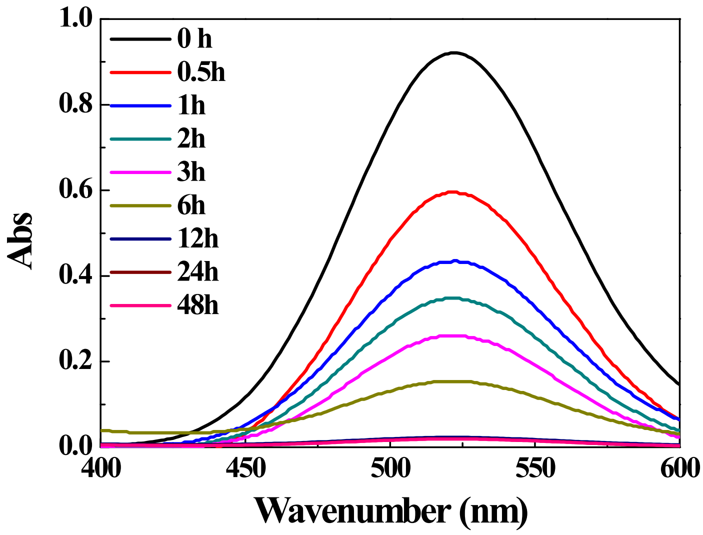

Fig. S6 UV-Vis spectra of iodine in hexane at different adsorption time for IL@PCN-333(Al).

Table S2 (a) Pseudo-first-order and (b) pseudo-second-order diffusion model plots for the iodine adsorption onto IL@PCN-333(Al) in hexane

	Pseudo-first-order model			Pseudo-second-order model		
C $mg\cdot L^{-1}$	q_e $mg\cdot g^{-1}$	k_1 min^{-1}	R^2	q_e $mg\cdot g^{-1}$	k_2 $g\cdot mg^{-1}\cdot min^{-1}$	R^2
1600	1250	0.00488	0.92316	1500	6.98E-04	0.99955

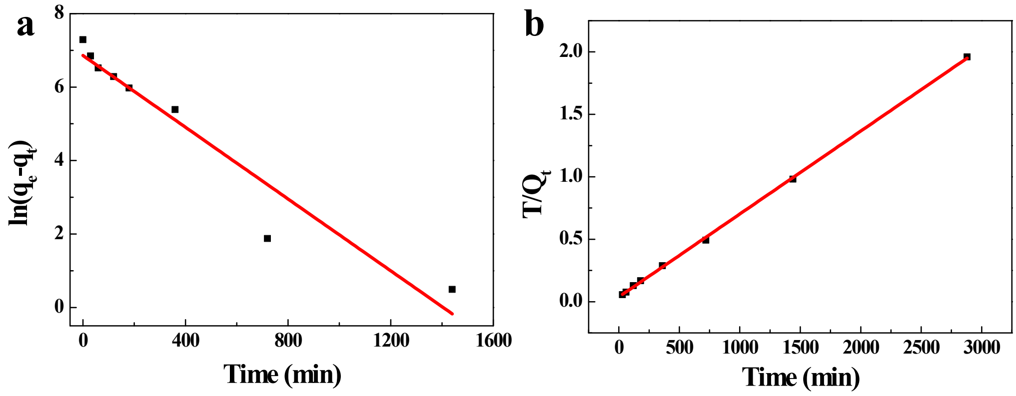

Fig. S7 Kinetic parameters for the iodine adsorption onto IL@PCN-333(Al) in hexane.

Table S3 Comparison of iodine solution adsorption in different materials.

No.	Name	BET surface area (m^2/g)	Pore volume (cc/g)	I_2 uptake(g/g)	*Ref.*
1	NTP	1067	-	0.429	*16*
2	SCMP-2	855	1.5	0.184	*17*
3	SCMP-1	413	0.23	0.145	*17*
4	NiP-CMP	2630	2	0.326	*19*
5	SCMP-II	119.76	0.61	0.324	*25*
6	MelTOP-2	50.5	0.22	1.239	*32*
7	TatPOP-2	36.5	0.18	0.764	*32*
8	AzoPPN	400	0.68	0.735	*33*
9	NOP-53	744	0.73	0.86	*34*
10	NOP-54	1178	1.32	0.89	*34*
11	NOP-55	526	0.42	0.81	*34*
12	AK-2	2751	1.34	0.336	*35*
13	3D-PPy	16	-	0.225	*36*
14	FCMP-600@1	551	0.3865	0.55	*44*
15	FCMP-600@2	636	0.6983	0.729	*44*
16	FCMP-600@3	692	0.4074	0.52	*44*
17	FCMP-600@4	88	0.118	0.539	*44*
18	NT-POP@800-2	630	0.433	1.191	*45*
19	NT-POP@800-3	475	0.187	0.97	*45*
20	NT-POP@800-4	736	0.463	1.202	*45*
21	MBM	62	0.624	0.88	*51*
22	SIOC-COF-7	618	0.41	0.127	*52*
23	JLNU-4	64	-	0.68	*61*
24	HCPs	584	0.41	0.167	*62*

25	HCOF-1	-	-	2.1	*64*
26	BC@Dopa-ZIF	1453	-	1.31	*65*
27	Cu/MIL-101	2264	1.04	0.432	*3*
28	MIL-101	3134	1.52	0.385	*3*
29	JLU-Liu32	1700	0.85	0.2	*66*
30	CP5	-	-	0.435	*67*
31	JLU-Liu14	-	-	0.5	*68*
32	Fe3O4@PPy	-	-	1.627	*69*
33	C@ETS-10	-	-	0.042	*70*
34	UiO-66-PYDC	1030	0.43	1.25	*71*
35	UiO-66	1015	0.5	0.401	*71*
36	Fe_3O_4/COF-5d	872	0.45	0.797	*72*
37	COF-5d	1500	0.77	0.91	*72*
38	HMTI-1	-	-	1.5	*73*
39	nano-HMTI-1	-	-	0.8	*73*
40	D201	-	-	0.256	*74*
41	Ag-D201	-	-	0.313	*74*
42	**IL@PCN-333(Al)**	**1635.3**	**1.40**	**3.4**	***This work***

Table. S4 Linearized Langmuir isotherms and Freundlich isotherms for iodine adsorption on IL@PCN-333(Al).

	Langmuir isotherm			**Freundlich isotherm**		
	Q_m (g/g)	**K_L (mL/mg)**	**R^2**	**k_F(g/g)**	**n**	**R^2**
IL@PCN-333(Al)	3.4	0.29762	0.98419	1	1.0036	0.99998

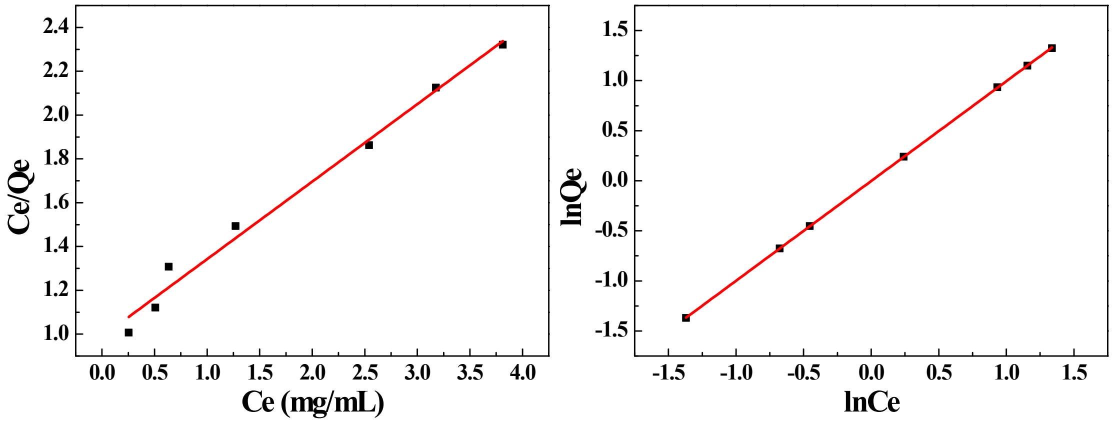

Fig. S8 Isotherms parameters for the iodine adsorption onto IL@PCN-333(Al) in hexane.

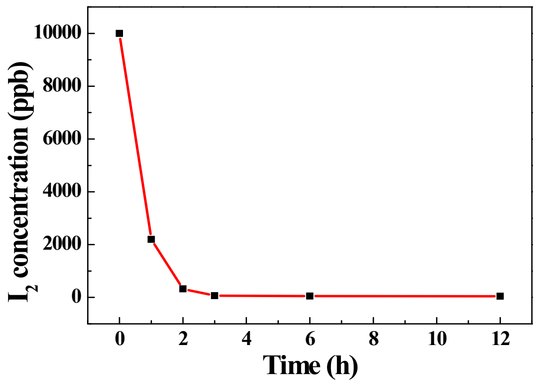

Fig. S9 Iodine adsorption kinetics of IL@PCN-333(Al) with iodine initial concentration of 10 ppm.

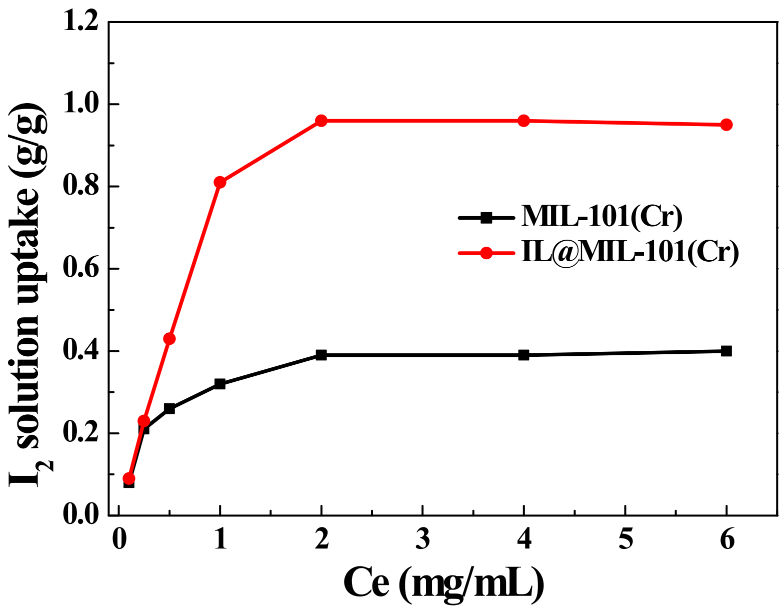

Fig. S10 Adsorption isotherm of iodine by dispersing 10 mg of adsorbents in 10 mL iodine-hexane solution for 48 h.

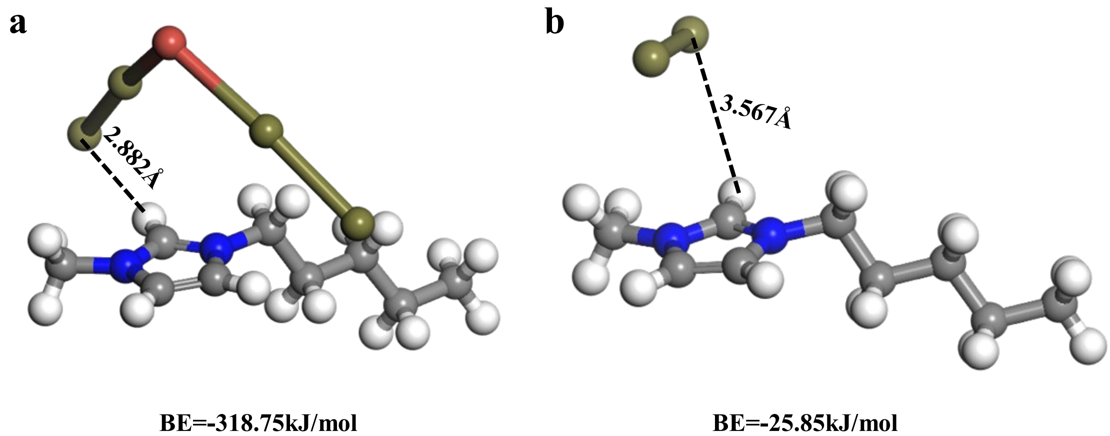

Fig. S11 Optimized geometries for the interactions of (a) I_4Br^- anion and (b) I_2 molecule with imidazole cations of the IL.

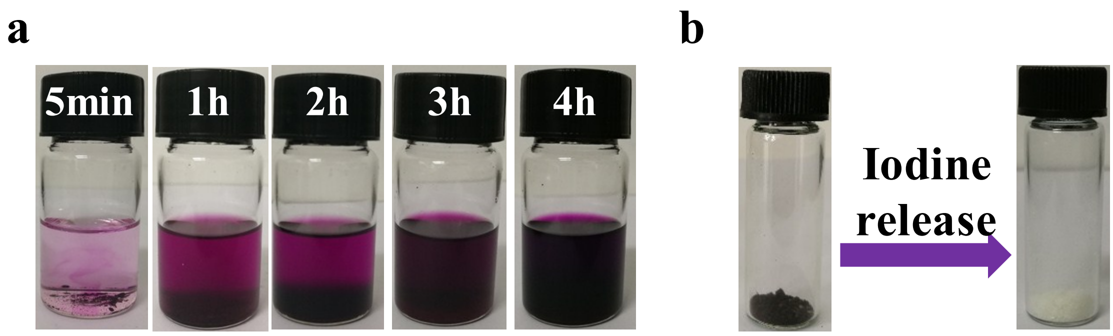

Fig. S12 Photographs of (a) I_2-IL@PCN-333(Al) in n-hexane at different contacting time and (b) I_2-IL@PCN-333(Al) before and after washing with n-hexane several times.

Reference

[1] D. W. Feng, K. C. Wang, J. Su, T. -F. Liu, J. Park, Z. W. Wei, M. Bosch, A. Yakovenko, X. D. Zou, and H. –C. Zhou, *Angew. Chem. Int. Ed.,* 2015, **54**, 149 –154.

[2] D. W. Feng, T. F. Liu, J. Su, M. Bosch, Z. W. Wei, W. Wan, D. Q. Yuan, Y. P. Chen, X. Wang, K. C. Wang, X. Z. Lian, Z. Y. Gu, J. Park, X. D. Zou and H. C. Zhou, *Nat. Commun.,* 2015, **6**, 5979.

[3] B. B. Qia, Y. Liu, T. Zheng, Q. H. Gao, X. W. Yan, Y. Jiao and Y. Yang, *J. Solid. State. Chem.,* 2018, **258**, 49-55.

[4] M. J. Frisch, G. W.Trucks, H. B. Schlegel, G. E. Scuseria, M. A. Robb, J. R. Cheeseman, J. A., Jr. Montgomery, T. Vreven, K. N. Kudin, J. C. Burant, J. M. Millam, S. S. Iyengar, J. Tomasi, V. Barone, B. Mennucci, M. Cossi, G. Scalmani, N. Rega, G. A. Petersson, H. Nakatsuji, M. Hada, M. Ehara, K. Toyota, R. Fukuda, J. Hasegawa, M. Ishida, T. Nakajima, Y. Honda, O. Kitao, H. Nakai, M. Klene, X. Li, J. E. Knox, H. P. Hratchian, J. B. Cross, V. Bakken, C. Adamo, J. Jaramillo, R. Gomperts, R. E. Stratmann, O. Yazyev, A. J. Austin, R. Cammi, C. Pomelli, J. W. Ochterski, P. Y. Ayala, K. Morokuma, G. A. Voth, P. Salvador, J. J. Dannenberg, V. G. Zakrzewski, S. Dapprich, A. D. Daniels, M. C. Strain, O. Farkas, D. K. Malick, A. D. Rabuck, K. Raghavachari, J. B. Foresman, J. V. Ortiz, Q. Cui, A. G. Baboul, S. Clifford, J. Cioslowski, B. B. Stefanov, G. Liu, A. Liashenko, P. Piskorz, I. Komaromi, R. L. Martin, D. J. Fox, T. Keith, M. A. Al-Laham, C. Y. Peng, A. Nanayakkara, M. Challacombe, P. M. W. Gill, B. Johnson, W. Chen, M. W. Wong, C. Gonzalez and J. A. Pople, Gaussian 03, revision D.01; Gaussian, Inc.: Wallingford, CT, 2004.

[5] D. Shetty, J. Raya, D. S. Han, Z. Asfari, J. C. Olsen and A. Trabolsi, *Chem. Mater.,* 2017, **29**, 8968-8972.

[6] Y. F. Chen, H. X. Sun, R. X. Yang, T. T. Wang, C. J. Pei, Z. T. Xiang, Z. Q. Zhu, W. D. Liang, A. Li and W. Q. Deng, *J. Mater. Chem. A.,* 2015, **3**, 87-91.

[7] D. Shetty, T. Skorjanc, J. Raya, S. K. Sharma, I. Jahovic, K. Polychronopoulou, Z. Asfari, D. S. Han, S. Dewage, J. C. Olsen, R. Jagannathan, S. Kirmizialtin and A. Trabolsi, *ACS Appl. Mater. Interfaces.,* 2018, **10**, 17359-17365.

[8] D. F. S. Gallis, I. Ermanoski, J. A. Greathouse, K. W. Chapman and T. M. Nenoff, *Ind. Eng. Chem. Res.,* 2017, **56**, 2331-2338.

[9] X. R. Zhang, I. D. Silva, H. G. W. Godfrey, S. K. Callear, S. A. Sapchenko, Y. Q. Cheng, I. V. Yrezabal, M. D. Frogley, G. Cinque, C. C. Tang, C. Giacobbe, C. Dejoie, S. Rudic, A. J. Ramirez-Cuesta, M. A. Denecke, S. H. Yang and M. Schröder, *J. Am. Chem. Soc.,* 2017, **139**, 16289-16296.

[10] L. Lin, H. D. Guan, D. L. Zou, Z. J. Dong, Z. Liu, F. F. Xu, Z. G. Xie and Y. X. Li, *RSC Adv.,* 2017, **7**, 54407-54415.
[11] S. L. Ma, S. M. Islam, Y. Shim, Q. Y. Gu, P. L. Wang, H. Li, G. B. Sun, X. J. Yang and M. G. Kanatzidis, *Chem. Mater.,* 2014, **26**, 7114-7123.
[12] Y. L. Zhu, Y. J. Ji, D. G. Wang, Y. Zhang, H. Tang, X. R. Jia, M. Song, G. P. Yu and G. C. Kuang, *J. Mater. Chem. A.,* 2017, **5**, 6622-6629.
[13] T. M. Geng, W. Y. Zhang, Z. M. Zhu, G. F. Chen, L. Z. Ma, S. N. Ye and Q. Y. Niu, *Polym. Chem.,* 2018, **9**, 777-784.
[14] Y. Z. Liao, J. Weber, B. M. Mills, Z. H. Ren and C. F. J. Faul, *Macromolecules*., 2016, **49**, 6322-6333.
[15] D. F. Sava, K. W. Chapman, M. A. Rodriguez, J. A. Greathouse, P. S. Crozier, H. Y. Zhao, P. J. Chupas and T. M. Nenoff, *Chem. Mater.,* 2013, **25**, 2591-2596.
[16] H. Ma, J. J. Chen, L. X. Tan, J. H. Bu, Y. H. Zhu, B. Tan and C. Zhang, *ACS Macro Lett.,* 2016, **5**, 1039-1043.
[17] X. Qian, Z. Q. Zhu, H. X. Sun, F. Ren, P. Mu, W. D. Liang, L. H. Chen and A. Li, *ACS Appl. Mater. Interfaces*., 2016, **8**, 21063-21069.
[18] Y. H. Abdelmoaty, T. D. Tessema, F. A. Choudhury, O. M. El-Kadri and H. M. El-Kaderi, *ACS Appl. Mater. Interfaces*., 2018, **10**, 16049-16058.
[19] A. Sigen, Y. W. Zhang, Z. P. Li, H. Xi, M. Xue, X. M. Liu and Y. Mu, *Chem. Commun.,* 2014, **50**, 8495-8498.
[20] K. S. Subrahmanyam, D. Sarma, C. D. Malliakas, K. Polychronopoulou, B. J. Riley, D. A. Pierce, J. Chun and M. G. Kanatzidis, *Chem. Mater.,* 2015, **27**, 2619-2626.
[21] Z. K. Yan, Y. Yuan, Y. Y. Tian, D. M. Zhang and G. S. Zhu, *Angew. Chem. Int. Ed.,* 2015, **54**, 12733-12737.
[22] P. Wang, Q. Xu, Z. P. Li, W. M. Jiang, Q. H. Jiang and D. L. Jiang, *Adv. Mater.,* 2018, 1801991.
[23] H. Li, X. S. Ding and B. H. Han, *Chem. Eur. J.,* 2016, **22**, 11863-11868.
[24] T. M. Geng, S. N. Ye, Z. M. Zhu and W. Y. Zhang, *J. Mater. Chem. A.,* 2018, **6**, 2808-2816.
[25] F. Ren, Z. Q. Zhu, X. Qian, W. D. Liang, P. Mu, H. X. Sun, J. H. Liu and A. Li, *Chem. Commun.,* 2016, **52**, 9797-9800.
[26] X. Qian, B. Wang, Z. Q. Zhu, H. X. Sun, F. Ren, P. Mu, C. H. Ma, W. D. Liang and A. Li, *J. Hazard. Mater.,* 2017, **338**, 224-232.

[27] X. H. Guo, Y. Tian, M. C. Zhang, Y. Li, R. Wen, X. Li, X. F. Li, Y. Xue, L. J. Ma, C. Q. Xia and S. J. Li, *Chem. Mater.,* 2018, **30**, 2299-2308.
[28] T. M. Geng, Z. M. Zhu, W. Y. Zhang and Y. Wang, *J. Mater. Chem. A.,* 2017, **5**, 7612-7617.
[29] C. Wang, Y. Wang, R. Ge, X. D. Song, X. Q. Xing, Q. K. Jiang, H. Lu, C. Hao, X. W. Guo, Y. N. Gao and D. L. Jiang, *Chem. Eur. J.,* 2018, **24**, 585-589.
[30] Y. Z. Liao, Z. H. Cheng, W. W. Zuo, A. Thomas and C. F. J. Faul, *ACS Appl. Mater. Interfaces.,* 2017, **9**, 38390-38400.
[31] Y. Li, W. B. Chen, W. J. Hao, Y. S. Li and L. Chen, *ACS Appl. Nano Mater., 2018*, **1**, 4756-4761.
[32] S. H. Xiong, J. Tao, Y. Y. Wang, J. T. Tang, C. Liu, Q. Q. Liu, Y. Wang, G. P. Yu and C. Y. Pan, *Chem. Commun.,* 2018, **54**, 8450-8453.
[33] G. Das, T. Skorjanc, S. K. Sharma, F. Gandara, M. Lusi, D. S. S. Rao, S. Vimala, S. K. Prasad, J. Raya, D. S. Han, R. Jagannathan, J. C. Olsen and A. Trabolsi, *J. Am. Chem. Soc.,* 2017, **139**, 9558-9565.
[34] D. Y. Chen, Y. Fu, W. G. Yu, G. P. Yu and C. Y. Pan, *Chem. Eng. J.,* 2018, **334**, 900-906.
[35] H. X. Sun, P. Q. La, R. X. Yang, Z. Q. Zhu, W. D. Liang, B. P. Yang, A. L and W. Q. Deng, *J. Hazard. Mater.,* 2017, **321***,* 210-217.
[36] P. Mu, H. X. Sun, T. Chen, W. L. Zhang, Z. Q. Zhu, W. D. Liang and A. Li, *Macromol. Mater. Eng.,* 2017, **302**, 1700156.
[37] B. X. Guo, S. J. Wu, Q. Su, W. T. Liu, P. Y. Ju, G. H. L and Q. L. Wu, *Materials Letters.,* 2018, **229***,* 240-243.
[38] T. M. Geng, W. Y. Zhang, Z. M. Zhu and X. M. Kai, *Micropor. Mesopor. Mat.,* 2019, **273**, 163-170.
[39] Q. Q. Dang, X. M. Wang, Y. F. Zhan and X. M. Zhang, *Polym. Chem.,* 2016, **7**, 643-647.
[40] B. Valizadeh, T. N. Nguyen, B. Smit and K. C. Stylianou, *Adv. Funct. Mater.,* 2018, **28**, 1801596.
[41] X. M. Zhang, C. W. Zhao, J. P. Ma, Y. Yu, Q. K. Liu and Y. B. Dong, *Chem. Commun.,* 2015, **51**, 839-842.
[42] K. C. Jie, H. Chen, P. F. Zhang, W. Guo, M. J. Li, Z. Z. Yang and S. Dai, *Chem. Commun.,* 2018, **54**, 12706-12709.
[43] Q. Jiang, H. L. Huang, Y. Z. Tang, Y. X. Zhang and C. L. Zhong, *Ind. Eng. Chem. Res.,* 2018, **57**, 15114-15121.
[44] G. Y. Li, C. Yao, J. K. Wang and Y. H. Xu, *Sci. Rep.,* 2017**,** **7**, 13972.

[45] C.Yao, G. Y. Li, J. K. Wang, Y. H. Xu and L. M. Chang, *Sci. Rep.,* 2018, **8**, 1867.
[46] M. H. Liu, C. Yao, C. B. Liu and Y. H. Xu, *Sci. Rep.,* 2018**, 8**, 14071.
[47] M. H. Liu, C.Yao, C. B. Liu and Y. H. Xu, *Sci. Rep.,* 2018, **8**, 14072.
[48] M. S. Deshmukh, A. Chaudhary, P. N. Zolotarev and R. Boomishankar, *Inorg. Chem.,* 2017, **56**, 11762-11767.
[49] K. S. Subrahmanyam, C. D. Malliakas, D. Sarma, G. S. Armatas, J. S. Wu and M. G. Kanatzidis, *J. Am. Chem. Soc.,* 2015, **137**, 13943-13948.
[50] K. Z. Su, W. J. Wang, B. B. Li and D. Q. Yuan, *ACS Sustainable Chem. Eng.,* 2018, **6**, 17402-17409.
[51] T. He, X. B. Xu, B. Ni, H. F. Lin, C. Z. Li, W. P. Hu and X. Wang, *Angew. Chem.,* 2018, **130**, 10305-10309.
[52] Z. J. Yin, S. Q. Xu, T. G. Zhan, Q. Y. Qi, Z. Q. Wu and X. Zhao, *Chem. Commun.,* 2017, **53**, 7266.
[53] J. Y. Yang, X. Feng, G. N. Lu, Y. L. Li, C. C. Mao, Z. L. Wen and W. B. Yuan, *Dalton Trans.,* 2018, **47**, 5065-5071.
[54] R. X. Yao, X. Cui, X. X. Jia, F. Q. Zhang and X. M. Zhang, *Inorg. Chem.,* 2016, **55**, 9270-9275.
[55] Z. D. He, T. Q. Wang, Y. Xu, M. H. Zhou, W. Yu, B. Y. Shi and K. Huang, *Polym. Sci. Part A: Polym. Chem.,* 2018, **56**, 2045-2052.
[56] T. M. Geng, G. F. Chen, H. Y. Xia, W. Y. Zhang, Z. M. Zhu and B. S. Cheng, *J. Solid. State., Chem.,* 2018, **265**, 85-91.
[57] X. M. Li, G. Chen and Q. Jia, *J. Taiwan. Inst. Chem. E.,* 2018, **000**, 1-7.
[58] G. Mehlana, G. Ramon and S. A. Bourne, *Micropor. Mesopor. Mat.,* 2016, **231**, 21-30.
[59] B. J. Riley, J. Chun, J. V. Ryan, J. Matya´sˇ, X. H. S. Li, D. W. Matson, S. K. Sundaram, D. M. Strachan and J. D. Vienna, *RSC Adv.,* 2011, **1**, 1704-1715.
[60] K. C. Park, J. Cho and C. Y. Lee, *RSC Adv.,* 2016, **6**, 75478-75481.
[61] C. Yao, W. Wang, S. R. Zhang, H. Y. Li, Y. H. Xu, Z. M. Su and G. B. Che, *RSC Adv.,* 2018, **8**, 36400-36406.
[62] X. M. Li, G. Chen, J. T. Ma and Q. Jia, *Sep. Purif. Technol.,* 2019, **210**, 995-1000.
[63] H. X. Sun, P. Mu, H. M. Xie, Z. Q. Zhu, W. D. Liang, Z. F. Zhou and A. Li, *ChemistrySelect.,* 2018, **3**, 10147-10152.
[64] Y. X. Lin, X. F. Jiang, S. T. Kim, S. B. Alahakoon, X. S. Hou, Z. Y. Zhang, C. M. Thompson, R. A. Smaldone and C. F. Ke, *J. Am. Chem. Soc.,* 2017, **139**, 7172-7175.
[65] A. Au-Duong and C. K. Lee, *Cryst. Growth Des.,* 2018, **18**, 356-363.

[66] S. Yao, X. D. Sun, B. Liu, R. Krishna, G. H. Li, Q. S. Huo and Y. L. Liu, *J. Mater. Chem. A.,* 2016, **4**, 15081-15087.
[67] P. Dastidar and S. Mondal, *Cryst. Growth Des.,* 2019, **19**, 470-478.
[68] J. Wang, J. H. Luo, X. L. Luo, J. Zhao, D. S. Li, G. H. Li, Q. S. Huo and Y. L. Liu, *Cryst. Growth Des.,* 2015, **15**, 915-920.
[69] D. K. L. Harijan, V. Chandra, T. Yoo and K. S. Kim, *J. Hazard. Mater.,* 2018, **344**, 576-584.
[70] S. U. Nandanwa, K. Coldsnow, A. Porter, P. Sabharwal, D. E. Aston, D. N. McIlroy and V. Utgikar, *Chem. Eng. J.,* 2017, **320**, 222-231.
[71] Z. Wang, Y. Huang, J. Yang, Y. S. Li, Q. X. Zhuang and J. L. Gu, *Dalton Trans.,* 2017, **46**, 7412-7420.
[72] Y. Z. Liao, J. H. Li and A. Thomas, *ACS Macro Lett.,* 2017, **6**, 1444-1450.
[73] L. Hashemi and A. Morsali, *CrystEngComm.,* 2012, **14**, 779-781.
[74] J. Li, M. X. Wang, G. C. Liu, L. Zhang, Y. L. He, X. Xing, Z. Qian, J. Z. Zheng and C. B. Xu, *Ind. Eng. Chem. Res.,* 2018, **57**, 17401-17408.